

MEMS based metal oxide sensor for simultaneous measurement of gas induced changes of the heating power and the sensing resistance

B. Bierer¹ · J. Kneer¹ · J. Wöllenstein¹ · S. Palzer¹

Received: 7 August 2015 / Accepted: 27 January 2016 / Published online: 4 February 2016
© Springer-Verlag Berlin Heidelberg 2016

Abstract Metal oxide based gas sensors are usually read-out by measuring the overall resistivity of the gas sensitive layer. However, the reaction of the gas species with the metal oxide surface does not only change the electrical conductivity but also effects the required heating power to maintain the layer's temperature. This change in power consumption may be disregarded when using standard bulk sensor chips due to their overall high thermal mass. Nevertheless, micromachined Si based hotplate devices offer the possibility to measure these effects. Here we present results that have been obtained by using a novel hotplate platform optimized for low power consumption and inkjet printing of nano sized gas sensitive metal oxide particles. The temperature of the gas sensitive layer is controlled via the heater resistance and the power consumption is recorded with a fully automated gas measurement system. To separate changes in the heat conductivity of the gas matrix from the heat of the surface reaction, the measurements have been performed in parallel using hotplates with and without a metal oxide layer deposited onto them. Here layers composed of copper (II) oxide have been used to highlight the possibilities of the novel approach. Determining both, the gas dependent resistivity as well as heating power yields two independent sensing quantities from one single device and might be an important cornerstone on the way towards selective metal oxide based gas sensors.

1 Introduction

Metal oxide layers have a long standing history as gas sensitive material (Heiland 1954) and are subject to intense research ever since. The sensing principle of metal oxide gas detectors is based on the gas induced changes of the electrical resistance (Williams 1999). While n-type semiconducting metal oxides are still at the center of attention, research of p-type semiconductors is recently enjoying an increased interest due to their specific features when used as gas sensitive materials, e.g. the possibility for low temperature operation (Barsan et al. 2010). In particular, pure copper (II) oxide (CuO) offers intriguing possibilities, e.g. for the detection of nitrogen dioxide (Li et al. 2008) (NO₂) and hydrogen sulfide (Kneer et al. 2014a) (H₂S). The gas sensitive properties of CuO can be further tailored by employing differently shaped CuO nanoparticles (Volanti et al. 2013) as well as by using different deposition techniques like sputtering (Frietsch et al. 2000), evaporation (Espinos et al. 2002), spray pyrolysis (Morales et al. 2005) or pulsed laser deposition (Chen et al. 2009). Both historically as well as commercially CuO has been investigated for its role in SnO₂/CuO heterostructures (Chowdhuri et al. 2004; Yamazoe 1991). In order to combine the vast possibilities of nano particle fabrication with the hotplate technology, inkjet printing offers unique possibilities as it enables high flexibility and contactless, precise deposition of arbitrary patterns of metal oxide particles (Sahner and Tuller 2010). With the resulting metal oxide micro hotplate sensors it is possible to measure alterations in the heating power consumption induced by either changes in the heat conductivity of the gas matrix or the reaction heat caused by the reaction between the gas species and the metal oxide surface.

✉ S. Palzer
stefan.palzer@imtek.uni-freiburg.de
<https://www.imtek.de/gassensoren>

¹ Laboratory for Gas Sensors, Department of Microsystems Engineering, University of Freiburg, Georges-Köhler-Allee 102, 79110 Freiburg, Germany

2 Hotplate sensor platform

In order to allow for measuring changes in the heating power a hotplate platform optimized to inkjet printing has been developed (Datasheet Fujifilm Dimatix DMP-2800 2013). The design offers a large interdigitated electrode area in comparison to the overall surface while ensuring a homogeneous temperature distribution among the gas sensitive layer. Fabrication of the platform is based on the Silicon-On-Insulator (SOI) technology featuring a device layer thickness of 4 μm and a front- and backside finish with a layer of 400 nm low-stress SiN. Metallization has been achieved by physical vapor deposition (sputtering) of tantalum and platinum (20 nm Ta/200 nm Pt) onto a structured SOI-wafer. The membrane was etched from the backside using a potassium hydroxide (KOH)-etch process. After this the silicon oxide was removed with a hydrofluoric acid (HF)-dip. Finally the membrane was opened with an inductively coupled plasma reactive ion etching (ICP-RIE) process. The membrane suspension has a total length of 550 μm and a width of 60 μm . A heating structure surrounds the interdigital electrodes in the center of the membrane. The membrane has an overall size of (600 \times 600) μm^2 and deposition of the gas sensitive layer onto the interdigitated area is achieved by a Dimatix DMP 2831 inkjet printing system with a minimum drop volume of 1 pL (Datasheet Fujifilm Dimatix DMP-2800 2013). This technique has been utilized in previous investigations by our group (Kneer et al. 2014a, 2016; Walden et al. 2015) and allows different printing patterns with a minimum drop volume of 1 pL. Furthermore, it is possible to control the layer thickness by printing various layers upon each other. Figure 1 shows a scanning electron microscopy (SEM) picture of a completely processed sensors chip. The hotplate is designed for low power consumption and fast temperature modulation but maintaining a homogenous temperature distribution along the membrane in order to acquire reliable data regarding the metal oxide performance. To allow for

separating effects of changes in the heat capacity of the gas matrix from the heat of surface reaction with gases a modified version of the sensor chip has been devised. There, the interdigitated structures has been connected such as to provide a resistance thermometer. A schematic of this design is shown in Fig. 1b.

Since both, the thermal loss processes as well as the temperature distribution among the hotplate are crucial for the evaluation of the experimental results a detailed thermal analysis using the finite element method (FEM) has been performed. Figure 2a shows a FEM simulation of the thermal distribution over the membrane featuring a high level of homogeneity of the temperature distribution along the interdigitated area. In the simulation the frame is kept fixed at room temperature (293 K). Figure 2b depicts the different contributions of the thermal loss mechanisms.

Both radiation and convection are negligible in the relevant temperature regime up to 450 $^{\circ}\text{C}$. The main loss mechanism at temperatures between 150 and 450 $^{\circ}\text{C}$ is thermal conduction through the suspension into the frame. Consequently, the thermal loss of the platform can be approximated as thermal conduction through the Si dominated suspension:

$$\dot{Q} = \frac{\kappa}{d} \cdot A \cdot (T_{HP} - T_{Frame}) \quad (1)$$

where the thermal conductivity κ has a value of 142 W/mK (Shanks et al. 1963) at 300 K for silicon, T_{HP} and T_{Frame} are the hotplate and frame temperatures, respectively, A describes the cross-sectional area of the suspension and d is the length of the suspension. Using thermally sensitive inks, the resistivity of the heating structure at different temperatures has been determined in order to achieve a temperature calibration of the hotplates which features an error of ± 4 K (Datasheet Fujifilm Dimatix DMP-2800 2013). This in turn enables a control of the hotplate temperature by controlling the heater current where the thermal power is generated through the ohmic losses of the platinum heating structure.

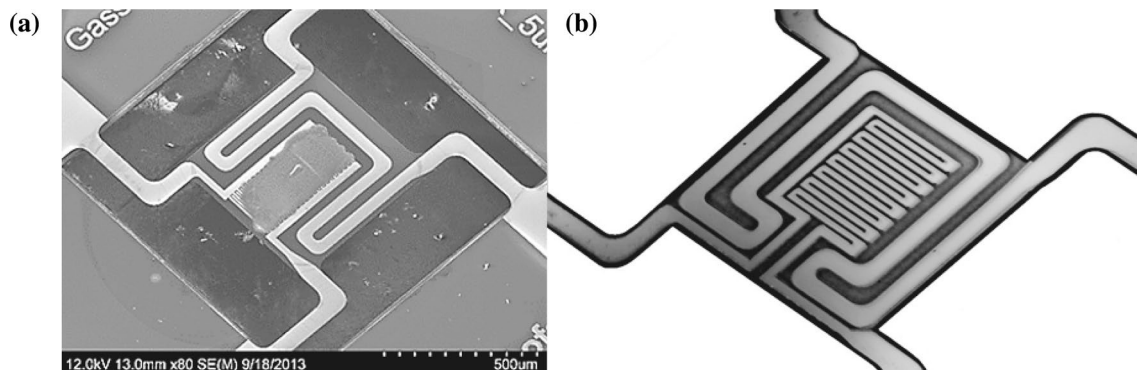


Fig. 1 **a** Scanning electron microscope image of a CuO layer inkjet deposited onto suspended micro hotplates. The interdigital electrodes are fully covered by CuO. **b** Image of a resistance thermometer with connected interdigital structures

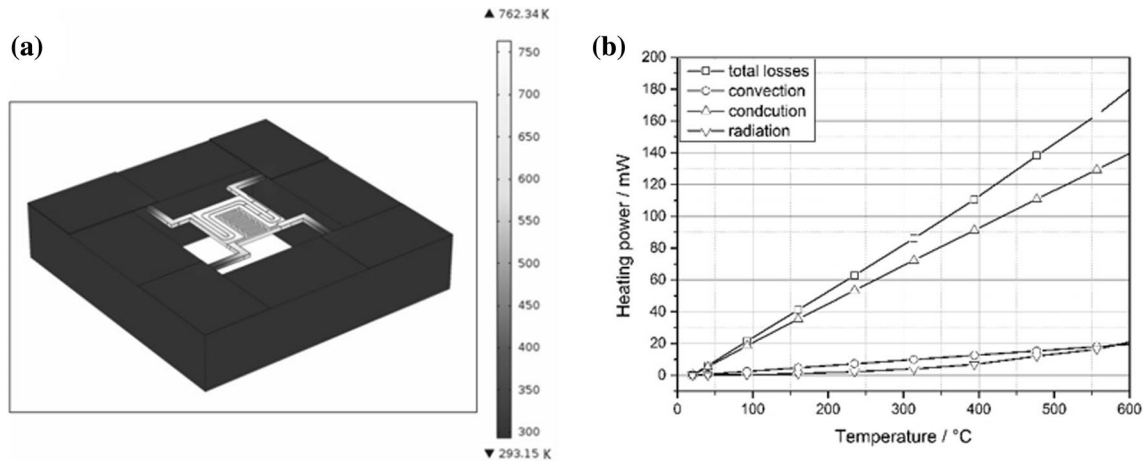


Fig. 2 **a** A thermal distribution simulation for the micro hotplate. The heat is uniformly distributed over the hotplate. Simulation results here are obtained at ~450 °C. The frame is kept on room temperature as a boundary condition. **b** Overview over the different heat loss

mechanisms. The conduction over the paths is dominating. The convection and the radiation are negligible for the temperature range from 150 to 450 °C

During measurements the temperature of each sensor chip is actively controlled through the fully automatic gas measuring system (Kneer et al. 2014b) and all parameters including the heating power consumption and the sensor resistance are recorded. This way it is possible to determine the power consumption for a fixed temperature.

3 Gas measurements

All measurements have been performed using a fully automatic gas measurement system. This apparatus can measure all relevant parameters of up to eight sensors simultaneously. This includes accurate control of the temperature as well as fast and precise read-out of the sensor resistance and heating power. A detailed description can be found in Kneer et al. (2014b). With this apparatus it is possible to set different humidity and oxygen levels in one measurement chamber as well as control the concentration of up to four trace gases. Thereby a lot of different conditions may be produced in order to simulate real-world situations. The measurements presented here aim at demonstrating how recording the heating power necessary to maintain a temperature may be used to increase the selectivity of metal oxide based gas sensors and provide additional information about the gas matrix. Furthermore, the measurements show that both, the heat capacity of a gas matrix as well as the reaction heat of the adsorption processes produce gaugeable effects.

3.1 Resistance control

For detecting the change in the power consumption the read-out of the heating resistance and the power

consumption needs to be fast and accurate. The sensors also have to react fast upon a change of the set temperature. This is done through the sensor design with its low thermal mass allowing for thermal modulation with frequencies >20 Hz. As a result the critical part of the system is the temperature control. Figure 3 shows a read-out of the preset heating resistance in comparison to the power consumption of the sensor.

In order to demonstrate the correct operation of the temperature stabilization protocol used here, the independent resistive thermometer shown in Fig. 1 has been used to validate the system’s readings (cf. Fig. 4a). Figure 3a shows the performance of the temperature stabilization for three different temperatures applied to the hotplate platform. The heater’s resistance and power consumption measurement was done in dry, synthetic air. The preset resistance was set to 148.9, 163.2 and 181.6 Ω. This correlates with a sensor temperature of 210, 290 and 400 °C, respectively. As shown in Fig. 3a the measured resistance varies only slightly around the set resistance. The inset shows the variation of the different measurement points during 8 min. The mean of the measurement points is $(163.19 \pm 0.034 \Omega)$, equivalent to a relative uncertainty of 0.021 %. The power consumption of the sensor, determined via the recorded heating current in the feedback loop, at this time is $(87.27 \pm 0.053 \text{ mW})$ which corresponds to a relative error of 0.1 %. After setting a new temperature a short overshoot in heating power consumption with a duration of 120 s is detected. Using this accurate measurement method it is possible to detect minimal changes in the power consumption of the sensor caused by changes in the gas composition. Taking the basic heater metallization calibration into account enables to derive the corresponding temperature

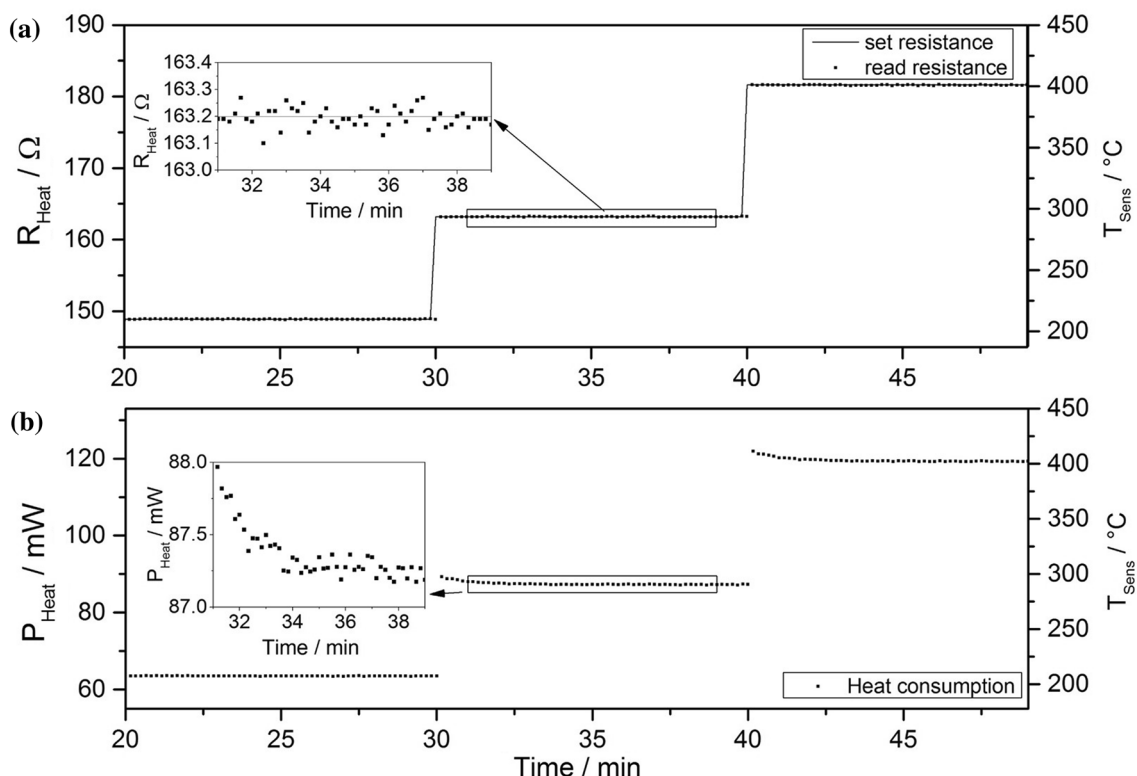


Fig. 3 **a** Three different preset heating resistances and the measured resistance. The difference between the set and the read resistance is very small. The *inset* shows the variation of the measured resistance.

The uncertainty is below one per mill. **b** The measurement of the heat consumption shows low variation. After the preset resistance was changed a short overshoot is detectable

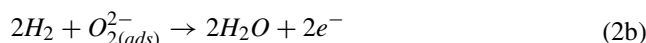
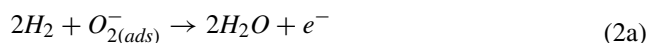
change, which has to be compensated by the heater, which is 4 K for a change in power consumption of 1 mW. Apart from the uncertainty introduced by the determination of the resistance no deviations from the set temperature are detected.

3.2 Hydrogen detection

For the cost-efficient detection of hydrogen (H_2) both thermal conductivity sensors as well as metal oxide gas sensors are well-suited and well described in literature (Buttner et al. 2011). However, both approaches exhibit cross-sensitivities towards other gases, limiting their informative value. On the one hand, thermal conductivity sensors are able to discriminate well between most gases and hydrogen but fail to separate helium and hydrogen. This is because the thermal conductivity coefficient of hydrogen (174 mW/m K at 298 K, 1 atm pressure) (Buttner et al. 2011) is close to that of helium (154 W/m K at 300 K, 1 bar pressure) (Petersen 1970). Both of them, however, feature a thermal conductivity at least five times higher than air under the same conditions (26 mW/m K) (Lemmon and Jacobsen 2004). On the other hand, metal oxide based gas sensors react similar to all reducing gas species, which makes it hard to distinguish

different reducing gases. Here, we present a combination of these sensor types combined in only one hotplate sensor. In order to demonstrate that the changes in heating power required to maintain the set temperature indeed stems from the changing thermal conductivity a reference sensor with a resistive thermometer has been employed in parallel during the measurements. The results of the experiments are shown in Fig. 4. The gas sensitive measurements were performed in dry synthetic air with hydrogen concentrations varying from 40 to 3000 ppm at 400 °C sensor temperature. The baseline resistance R_0 and primary power consumption P_0 are determined from the sensor characteristic in dry synthetic air, i.e. without gas interference.

Hydrogen increases the resistance of the CuO layer due to its behavior as a reducing gas according to the proposed surface reaction (Morrison 1987):



A low concentration of 40 ppm is well detectable through the rising electrical resistance as well as the changes in heating power required to maintain the temperature. The

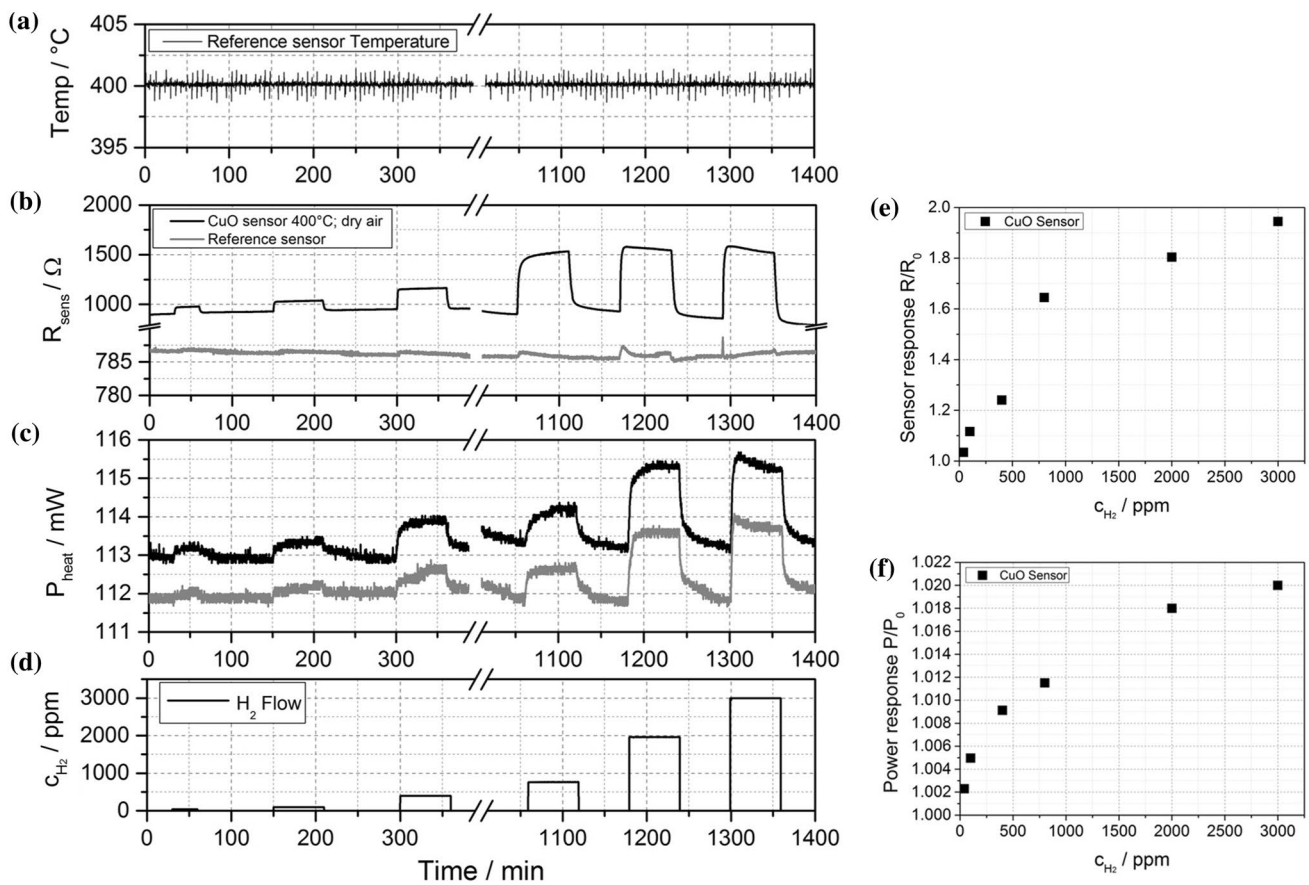


Fig. 4 **a** Recorded sensor temperature during the experiment. **b** Resistivity values of the CuO sensor and the reference resistive thermometer during increasing hydrogen exposure from 40 to 3000 ppm. The reference sensor shows no major gas specific change in the electrical resistance which means that the hotplate set-temperature remains constant. On the other hand, the resistivity of the CuO layer changes as a function of the gas concentration. **c** The heating power necessary to maintain the temperature increases for both sensors with

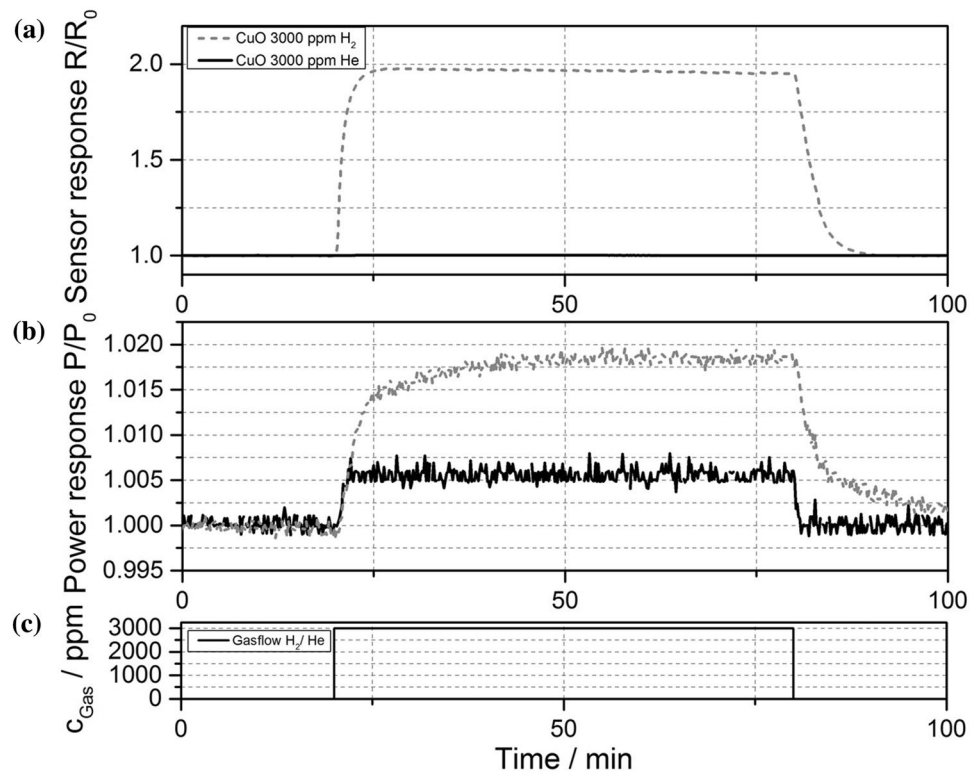
increasing H₂ concentration due to the larger heat transfer to the gas, a thermal response of 2.2 mW at 3000 ppm H₂ is observed. **d** At constant total gas flow the hydrogen concentrations are varied by mixing with dry synthetic air. **e** The sensor response R/R_0 is depicted for various hydrogen concentrations and reaches 1.95 for 3000 ppm H₂. **f** The corresponding changes in power consumption show a change of 2 % at 3000 ppm

sensor reacts with a fast response upon gas exposure and shows a small baseline drift with a sensor response of 1.22 at 400 ppm (Fig. 4e). To confirm the stable temperature operation a hotplate resistance thermometer (c.f. Fig. 1b) is used which shows no gas specific changes in response to the gas exposure, meaning that the temperature stabilization works as intended. The slight drift is forced due to the changes of the chamber temperature. Figure 4c shows the heating power of the CuO and the reference sensor. The heating power of both sensors differs slightly by about 1 mW which corresponds to a temperature difference of 4 K, i.e. within the uncertainty of the determination of the hotplate temperature. The heating power increases during hydrogen exposure both for the CuO and the reference sensor. At 400 ppm the power response of the metal oxide sensor is slightly higher than the blank one which potentially originates from the higher surface area of the metal oxide

enhancing the heat transfer. So the hydrogen concentration may be determined in a second way using the same device via the changing heat conductivity of the gas. The increase in heating power amounts to 0.9 mW, at 400 ppm hydrogen, what corresponds to a temperature change of 3.6 K. Even the small change of 0.2 mW, i.e. 0.8 K induced by 40 ppm H₂ is detectable with our approach. At 800 ppm the power difference has a value of 1 mW. At a hydrogen concentration of 3000 ppm the power consumption is 2.2 mW higher as compared to dry synthetic air. This reveals an increased power consumption of 2 %. After every gas exposure step the power consumption reaches the same values, i.e. the baseline is very stable indicating no changes in the micromachined Ta/Pt structures.

On the other hand, the resistivity of the CuO layer exhibits a small baseline drift. The normalized sensors response of the CuO layer is shown in Fig. 4e. The response has a value

Fig. 5 Comparison of the normalized CuO sensor responses towards hydrogen (dashed line) and helium (solid line) in purpose of better clarity **a** resistance response and **b** corresponding power response towards, **c** 3000 ppm of respective gas. Both gases provoke a significant change in power consumption. However, the absence of any resistance response towards He allows for a distinct discrimination



of 1.65 at 800 ppm and raises up to 1.95 at 3000 ppm. As depicted in Fig. 5, helium in comparison is not changing the resistivity of the CuO layer at all since it is chemically inert.

Figure 5 describes the difference in the sensor response of the highly thermal conductive gases hydrogen and helium. The experiments were carried out in equal conditions for both gases, i.e. in dry synthetic air with a concentration of 3000 ppm. As shown in Fig. 5a the CuO sensor has a distinct response towards H_2 while He is not inducing changes to the sensor resistance, as it was expected from its inert nature. Figure 5b reveals a power consumption increase by 2 % towards H_2 , while for Helium the power consumption increase is also distinct, yet with 0.5 % smaller than for hydrogen. Hence, combining both read-out techniques enables the selective and sensitive detection of hydrogen and helium in arbitrary gas mixtures.

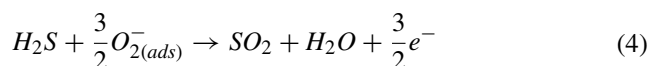
3.3 H_2S detection

Reading out the heating power may also be used to acquire information about surface heats yielding additional information to discriminate different trace gases. To highlight that possibility, we use the reaction of CuO towards hydrogen sulfide (H_2S), which is a very corrosive and toxic gas. Depending on the temperature regime H_2S converts CuO to CuS, allowing for a selective detection based on a percolation phase transition reaction that reduces the resistivity of the metal oxide layer by several orders of magnitude

(Kneer et al. 2014a). H_2S directly reacts with copper oxide to form copper sulfide (CuS) (Yuanda et al. 2001) at temperature below 200 °C according to:



This reaction competes with a second reaction that becomes dominant for temperature above 350 °C. The resistivity increases upon the exposure to H_2S according to the following reaction (Zhang et al. 2010):



Here, the adsorbed oxygen reacts with the hydrogen sulfide and releases electrons into the CuO layer. Figure 6a shows how the phase transition may be used to monitor the H_2S concentration by determining the time it takes for the CuO layer to become highly conductive in the low temperature regime.

The concentrations of H_2S are varied from 3 to 15 ppm in a dry synthetic air with an oxygen concentration of 20 %. As shown in Fig. 6a the reaction from CuO to CuS occurs quickly within seconds. E.g. the reaction from a semiconducting material to a layer featuring metallic conductivity values takes only 120 s for 4 ppm.

Figure 6c describes a typical sensor reaction (Eq. 4) at higher temperature where the phase transition does not occur. So the sensor temperature may be used as a tool to decide whether the phase transition takes place or not.

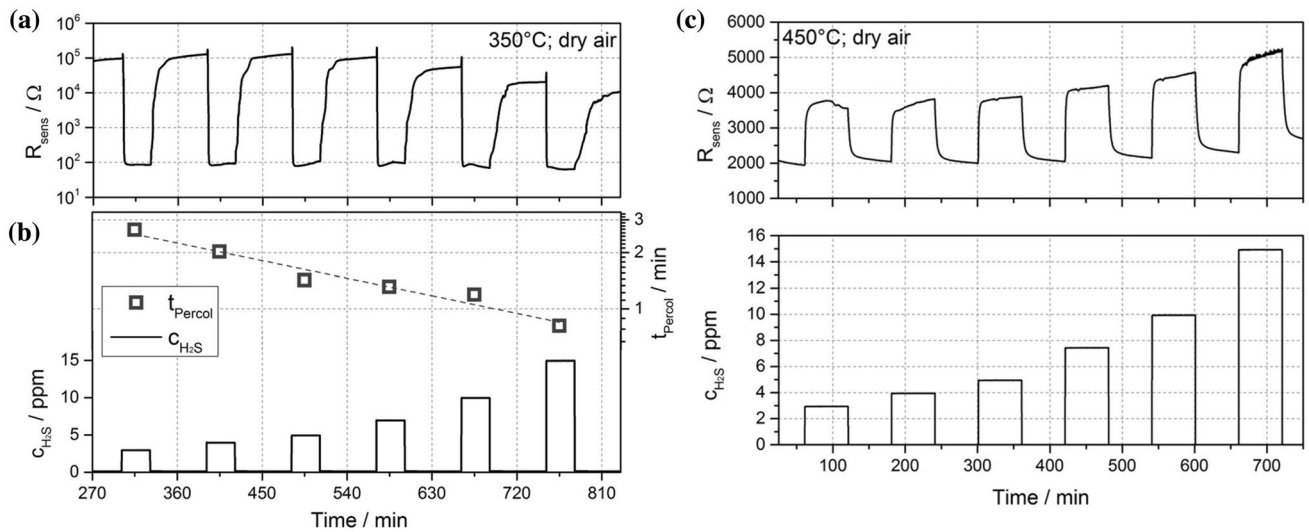


Fig. 6 **a** Sensor signal of the resistive metal oxide layer for the different concentrations shown in **b**. The percolation time correlates with the H₂S concentrations. **c** Increasing the temperature disables the

phase transition for the same hydrogen sulfide concentrations. The sensor reacts with a typical sensor response

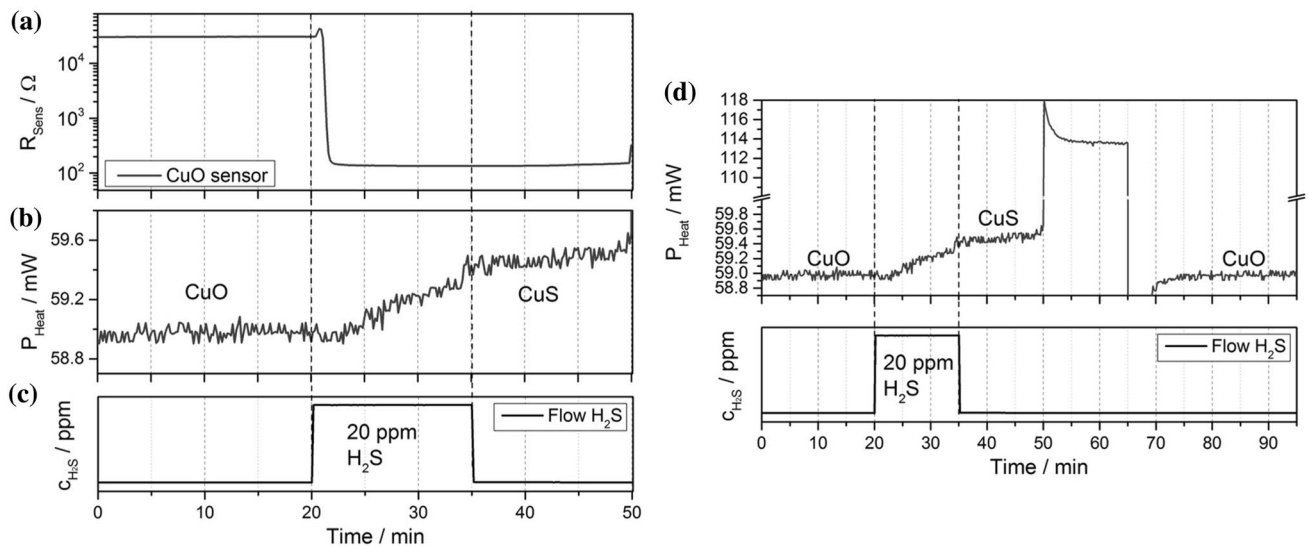


Fig. 7 **a** A percolation reaction from CuO to CuS is shown at 20 ppm H₂S in dry synthetic air at 200 °C sensor temperature. The steep drop in resistance heralds the phase transition. Even after removal of H₂S from the chamber, the electrical conductivity remains high which demonstrates the stability of the CuS structures at 200 °C. **b** While H₂S is flowing the heat consumption of the sensor increases once the

percolation phase transition has occurred. After the exposure the heating power stays on a new plateau due to its different thermal properties. **c** The H₂S concentration in the measurement chamber is set to 20 ppm for 15 min. **d** CuS could be transformed back to CuO due to a high temperature step at 400 °C. After that, the power consumption displays the full remove of the lattice sulfur

Figure 7a also shows a detailed view of the typical sensor reaction towards H₂S of the metal oxide layer.

If the adsorbed oxygen is depleted, H₂S reacts directly with lattice oxygen to form metallic copper sulfide. Once a conductive path along the surface has been formed, no further changes in the resistance are detected. However, taking a look at the heat consumption Fig. 7b reveals further changes in the material composition. The measurement is

performed at 200 °C in dry synthetic air. With the onset of the phase transition the heating power increases up until the point when H₂S is removed from the measurement chamber. Subsequently, the power consumption remains stable but about 0.9 % higher as compared to the initial conditions, i.e. it increases from 59 mW before the exposure to 59.5 mW after the exposure to H₂S. Here, we can neglect changes in the heat transfer mechanisms, as the thermal

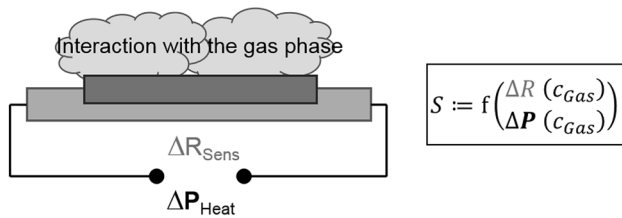


Fig. 8 Scheme of the sensing principle: By recording the heating power of the hotplate the power consumption is monitored as independent parameter thus making additional information available. The total sensor response (S) is comprised of the electrical resistance and the power consumption of the sensor

conductivity of H_2S is not elevated in contrary to hydrogen or helium. Presumably, the increase in power consumption is caused by the conversion of CuO to CuS which features a different heat capacity. For the given temperature the molar heat capacities ($c_{p,m}$) of CuO and CuS are 50.13 J/K mol (Leitner et al. 2000) and 52.21 J/K mol (Westrum et al. 1987) respectively. With the dimensions given in Sect. 1, we derive an estimation for the discrete heat capacity of the hot plate platform of $c_{p,HP} = 2.24 \mu\text{J/K}$ and for the active CuO layer a $c_{p,CuO}$ of $0.95 \mu\text{J/K}$. Assuming a full conversion to CuS gives $c_{p,CuS} = 0.99 \mu\text{J/K}$. Thus, the overall heat capacity changes with a maximum ratio R

$$R = (c_{p,HP} + c_{p,CuS}) / (c_{p,HP} + c_{p,CuO}) = 1.0125, \quad (5)$$

i.e. the heat capacity changes up to 1.25 %. With $E = c_p \cdot T$ it is obvious that, in order to maintain a set temperature, the energy input to the system has to increase alike, as we experimentally confirm here. Hence it becomes possible to monitor chemical conversion processes of a gas sensitive metal oxide layer via the heating power consumption. The stable higher power consumption indicates that CuS remains stable at $200 \text{ }^\circ\text{C}$ as opposed to the high temperature regime at $350 \text{ }^\circ\text{C}$ where CuS is converted back to CuO once the H_2S is removed. As displayed in Fig. 8d, the CuS can be converted back to CuO with an extra temperature step at $400 \text{ }^\circ\text{C}$, which corresponds to a heating power of 114 mW , for 15 min . After this, the power consumption has the same level as before the gas exposure. The sensor is perfectly reset and CuS is converted back to CuO . So the repeatability of this process could be shown both in the resistivity of the layer as well as in the heating power consumption.

These results demonstrate that by measuring the power consumption of hotplate devices a second, independent route to extract information about a gas composition may be accessed. The implementation does not require a change in the basic design of sensor devices but rather acquiring readily available data from the micromachined device. This approach is highlighted in Fig. 8 and may be employed to increase the selectivity of the metal oxide gas sensors.

4 Conclusion

In this manuscript we presented an approach to increase the selectivity of metal oxide based gas sensors. To this end a micromachined hotplate gas sensor featuring low power consumption and a small thermal mass was employed. Using this sensor platform it is possible to detect not only the electrical changes of the sensor due to the gas exposure but additionally measure the power consumption change caused by changes in the gas composition. We demonstrated the capabilities in using two exemplary cases.

Firstly, exploiting the high thermal conductivity of hydrogen as a selective criterion we demonstrated the selective detection of low levels of hydrogen. A small concentration of 40 ppm hydrogen shows detectable reactions in both independent sensor signals. At the other side of the scale even a concentration of 3000 ppm is detectable with both sensor signals. So the metal oxide gas sensor can be used for detection of hydrogen for almost three orders of magnitude. Contrasting measurement towards He additionally prove the selectivity of the method.

Secondly, we demonstrated that surface reactions may be detected using a hotplate platform. For this, the reaction between H_2S gas and CuO layers was used as sample system. Determining the heating power consumption revealed that the gas sensitive material and corresponding heat capacity changes upon H_2S exposure even after changes in the electrical conductivity are no longer detectable. Furthermore, at a temperature of $200 \text{ }^\circ\text{C}$ the change of the layer's composition is permanent and does not change even after the removal of H_2S from the gas measurement chamber. With an additional temperature step it is possible to reset the sensor and prepare it for the next measurements.

The results show that measuring the heating power may offer a versatile tool to increase the selectivity of metal oxide based gas sensors without the need to change the chip design. Additionally the measurement of the power consumption could be an indication whether the conversion from CuS to CuO has completely finished.

Acknowledgments This work was supported by a Grant from the German Federal ministry of Science and Education (BMBF) under Grant Number 16SV5943 (SensOdor). B.B. acknowledges funding by the graduate school “decentralized, sustainable energy systems (DENE)”.

References

- Barsan N, Simion C, Heine T, Pokhrel S, Weimar U (2010) Modeling of sensing and transduction for p-type semiconducting metal oxide based gas sensors. *J Electroceram* 25:11–19
- Buttner WJ, Post MB, Burgess R, Rivkin C (2011) An overview of hydrogen safety sensors and requirements. *Int J Hydrog Energy* 36(3):2462–2470

- Chen A, Long H, Li X, Li Y, Yang G, Lu P (2009) Controlled growth and characteristics of single-phase Cu_2O and CuO films by pulsed laser deposition. *Vacuum* 83(6):927–930
- Chowdhuri A, Gupta V, Sreenivas K, Kumar R, Mozumdar S, Patanjali PK (2004) Response speed of SnO_2 -based H_2S gas sensors with CuO nanoparticles. *Appl Phys Lett* 84:1180
- Datasheet Fujifilm Dimatix DMP-2800 (2013). <http://www.fujifilm-musa.com/shared/bin/PDS00085-DMP2831.pdf>. Date of access 30 Mar 2015
- Espinos JP, Morales J, Barranco A, Caballero A, Holgado JP, Gonzalez-Eliphe AR (2002) Interface effects for Cu , CuO , and Cu_2O deposited on SiO_2 and ZrO_2 . XPS determination of the valence state of copper in Cu/SiO_2 and Cu/ZrO_2 catalysts. *J Phys Chem B* 106:6921–6929
- Frietsch M, Zudock F, Goschnick J, Bruns M (2000) CuO catalytic membrane as selectivity trimmer for metal oxide gas sensors. *Sensors Actuators B Chem* 65:379–381
- Heiland G (1954) Zum Einfluß von adsorbiertem Sauerstoff auf die elektrische Leitfähigkeit von Zinkoxydkristallen. *Zeitschrift für Physik* 138(3–4):459–464
- Kneer J, Wöllenstein J, Palzer S (2014a) Specific, trace gas induced phase transition in copper(II)oxide for highly selective gas sensing. *Appl Phys Lett* 105:073509
- Kneer J, Eberhardt A, Walden P, Ortiz Pérez A, Wöllenstein J, Palzer S (2014b) Apparatus to characterize gas sensor response under real-world conditions in the lab. *Rev Sci Instrum* 85:055006
- Kneer J, Knobelspies S, Bierer B, Wöllenstein J, Palzer S (2016) New method to selectively determine hydrogen sulfide concentrations using CuO layers. *Sensors Actuators B Chem* 222:625–631
- Leitner J, Sedmidubsky D, Dousova B, Strejc A, Nevřiva M (2000) Heat capacity of CuO in the temperature range of 298.15–1300 K. *Thermochim Acta* 1–2:49–51
- Lemmon EW, Jacobsen RT (2004) Viscosity and thermal conductivity equations for nitrogen, oxygen, argon, and air. *Int J Thermophys* 25(1):21–69
- Li Y, Liang J, Tao Z, Chen J (2008) CuO particles and plates: synthesis and gas-sensor application. *Mater Res Bull* 43(8–9):2380–2385
- Morales J, Sánchez L, Martín F, Ramos-Barrado JR, Sánchez M (2005) Use of low-temperature nanostructured CuO thin films deposited by spray-pyrolysis in lithium cells. *Thin Solid Films* 474(1–2):133–140
- Morrison SR (1987) Selectivity in semiconductor gas sensors. *Sensors and Actuators* 12:425–440
- Petersen H (1970) The properties of helium: density, specific heats, viscosity, and thermal conductivity at pressures from 1 to 100 bar and from room temperature to about 1800 K. In: Riso Report No. 224
- Sahner K, Tuller HL (2010) Novel deposition techniques for metal oxide: prospects for gas sensing. *J Electroceram* 24:77–199
- Shanks HR, Maycock PD, Sidles PH, Danielson GC (1963) Thermal conductivity of silicon from 300 to 1400°K. *Phys Rev* 130:1743
- Volanti DP, Felix AA, Orlandi MO, Whitfield G, Yang D-J, Longo E, Tuller HL, Varela JA (2013) The role of hierarchical morphologies in the superior gas sensing performance of CuO -based chemiresistors. *Adv Funct Mater* 23:1759–1766
- Walden P, Kneer J, Knobelspies S, Kronast W, Mescheder U, Palzer S (2015) Micromachined hotplate platform for the investigation of ink-jet printed, functionalized metal oxide nanoparticles. *J Microelectromech* 24(5):1384–1390
- Westrum EF, Stolen S, Gronvold F (1987) Thermodynamics of copper sulfides II. Heat capacity and thermodynamic properties of synthetic covellite, CuS , from 5 to 780.5 K. Enthalpy of decomposition. *J Chem Thermodyn* 19:1199–1208
- Williams DE (1999) Semiconducting oxides as gas-sensitive resistors. *Sensors Actuators B Chem* 57(1–16):1–3
- Yamazoe N (1991) New approaches for improving semiconductor gas sensors. *Sensors Actuators B* 5:7–19
- Yuanda W, Maosong T, Xiuli H, Yushu Z, Guorui D (2001) Thin film sensors of SnO_2 - CuO - SnO_2 sandwich structure to H_2S . *Sensors Actuators B Chem* 79(2–3):187–191
- Zhang F, Zhu A, Luo Y, Tian Y, Yang J, Qin Y (2010) CuO nanosheets for sensitive and selective determination of H_2S with high recovery ability. *J Phys Chem C* 114(45):19214–19219